Supplemental Material

Suppressor analysis uncovers that MAPs and microtubule dynamics balance with the Cut7/Kinesin-5 motor for mitotic spindle assembly in *Schizosaccharomyces pombe*

Masashi Yukawa, Yusuke Yamada and Takashi Toda

Supplemental Table S1: Fission yeast strains used in this study

Strains	Genotypes	Figures used	Derivations
513	*h⁻ leu1 ura4*	1A, 1C-D, 4A, 5A-B, S1C, S7	Our lab stock
MY638	*h⁻ cut7-22 ade6-210*	1A, 1C-D, 4A	Our lab stock
YY60	*h⁻ cut7-22 skf1-7 (pkl1-E726D) ade6-210*	1A	This study
YY03	*h⁻ cut7-22 skf2-5 (wdr8-W399R) ade6-210*	1A	This study
MY1515	*h⁻ cut7-22 skf3-2 (msd1-L217FfsX4) ade6-210*	1A	This study
MY1472	*h⁻ cut7-22 skf4-1-kanR (nda3-G56D-kanR) ade6-210*	1A	This study
YY66	*h⁻ cut7-22 skf5-1 (atb2-G410A) ade6-210*	1A	This study
YY61	*h⁻ cut7-22 skf6-1 (mal3-K47KfsX4) ade6-210*	1A	This study
YY147	*h⁻ cut7-22 pkl1::natR leu1 ura4*	1C	This study
MY942	*h⁻ cut7-22 wdr8::natR ade6-210*	1C	This study
MY598	*h⁻ cut7-22 msd1::hphR leu1 ura4 ade6-210*	1C	This study
YY183	*h⁺ cut7-22 atb2::ura4⁺ leu1 ura4 his2*	1C	This study
YY214	*h⁻ cut7-22 mal3::ura4⁺ ura4*	1C	This study
YY251	*h⁻ cut7-22 alp16::ura4⁺ leu1 ura4*	1D	This study
YY163	*h⁻ cut7-22 klp2::hphR leu1 ura4*	1D	This study
YY177	*h⁻ cut7-22 alp7::hphR leu1 ura4*	1D	This study
MY1528	*h⁻ cut7-22 alp14::kanR leu1 ura4*	1D	This study
YY231	*h⁻ cut7-22 dis1::hphR leu1 ura4*	1D	This study
MY331	*h⁻ kanR-GFP-alp4 aur1R-Pnda3-mCherry-atb2 leu1 ura4*	1E-F, S4C-D	This study
MY652	*h⁻ cut7-22 kanR-GFP-alp4 aur1R-Pnda3-mCherry-atb2 leu1 ura4*	1E-F, 3A-C, S4A-D	This study
YY241	*h⁻ cut7-22 mal3:: kanR-GFP-alp4 aur1R-Pnda3-mCherry-atb2 leu1 ura4*	1E-F, 3C	This study
YY271	*h⁻ cut7-22 alp16::ura4⁺ kanR-GFP-alp4 aur1R-Pnda3-mCherry-atb2 leu1 ura4*	1E-F, 3C	This study
YY236	*h⁺ cut7-22 pkl1::natR kanR-GFP-alp4 aur1R-Pnda3-mCherry-atb2 leu1 ura4 his2*	1F, 3C	This study
MY1334	*h⁻ cut7-22 wdr8::natR kanR-GFP-alp4 aur1R-Pnda3-mCherry-atb2 leu1 ura4*	1F	This study
MY728	*h⁻ cut7-22 msd1::natR kanR-GFP-alp4 aur1R-Pnda3-mCherry-atb2 leu1 ura4 ade6-210*	1F	This study
MY1777	*h⁻ cut7-22 nda3-G56D-kanR kanR-GFP-alp4 aur1R-Pnda3-mCherry-atb2 leu1 ura4*	1F	This study
YY238	*h⁺ cut7-22 klp2::hphR kanR-GFP-alp4 aur1R-Pnda3-mCherry-atb2 leu1 ura4 his2*	1F, 3C	This study
MO51	*h⁻ cut7-22 alp7::hphR kanR-GFP-alp4 aur1R-Pnda3-mCherry-atb2 leu1 ura4*	1F	This study
MY1789	*h⁺ cut7-22 alp14::hphR kanR-GFP-alp4 aur1R-Pnda3-mCherry-atb2 leu1 ura4 his2*	1F	This study
MY1780	*h⁻ cut7-22 dis1::hphR kanR-GFP-alp4 aur1R-Pnda3-mCherry-atb2 leu1 ura4*	1F	This study

MY1030	*h⁻ kanR-Palp4-GFP-klp2 aur1R-Pnda3-mCherry-atb2 leu1 ura4*	2A-B, 4B-C	This study
MY1439	*h⁻ mal3::ura4+ kanR-Palp4-GFP-klp2 aur1R-Pnda3-mCherry-atb2 leu1 ura4*	2A-B	This study
MY1458	*h⁻ alp16::ura4+ kanR-Palp4-GFP-klp2 aur1R-Pnda3-mCherry-atb2 leu1 ura4*	2A-B	This study
MY1490	*h⁻ cut7-22 kanR-Palp4-GFP-klp2 aur1R-Pnda3-mCherry-atb2 leu1 ura4*	2B, 4B-C	This study
MY1489	*h⁺ cut7-22 mal3::ura4⁺ kanR-Palp4-GFP-klp2 aur1R-Pnda3-mCherry-atb2 leu1 ura4 his2*	2B	This study
MY1492	*h⁻ cut7-22 alp16::ura4⁺ kanR-Palp4-GFP-klp2 aur1R-Pnda3-mCherry-atb2 leu1 ura4*	2B	This study
MY1695	*h⁻ leu1 ura4* [pREP41-GFP]	2C, 4E	This study
MY1697	*h⁻ leu1 ura4* [pREP41-GFP-klp2]	2C, 4E	This study
MY1699	*h⁺ cut7-22 leu1 ura4 his2* [pREP41-GFP]	2C, 4E	This study
MY1701	*h⁺ cut7-22 leu1 ura4 his2* [pREP41-GFP-klp2]	2C, 4E	This study
MY1703	*h⁺ cut7-22 mal3::ura4⁺ leu1 ura4 his2* [pREP41-GFP]	2C	This study
MY1705	*h⁺ cut7-22 mal3::ura4⁺ leu1 ura4 his2* [pREP41-GFP-klp2]	2C	This study
MY1707	*h⁻ cut7-22 alp16::ura4⁺ leu1 ura4* [pREP41-GFP]	2C	This study
MY1709	*h⁻ cut7-22 alp16::ura4⁺ leu1 ura4* [pREP41-GFP-klp2]	2C	This study
MY844	*h⁻ cut11-GFP-ura4⁺ kanR-GFP-alp4 aur1R-Pnda3-mCherry-atb2 leu1 ura4*	3A-C, S4A-B	This study
MY1008	*h⁻ cut7-21 leu1 ura4*	4A	Our lab stock
MA2-3D	*h⁻ cut7-23 leu1*	4A	Our lab stock
IH136	*h⁻ cut7-24 leu1*	4A	Our lab stock
NK193	*h⁺ cut7-446 leu1 his2*	4A	Our lab stock
MY858	*h⁻ kanR-Palp4-GFP-pkl1 aur1R-Pnda3-mCherry-atb2 leu1 ura4*	4D, S3A-B	This study
MY1482	*h⁻ cut7-22 kanR-Palp4-GFP-pkl1 aur1R-Pnda3-mCherry-atb2 leu1 ura4*	4D, S3B	This study
YY305	*h⁻ leu1 ura4* [pREP41-GFP-pkl1]	4E	This study
YY308	*h⁺ cut7-22 leu1 ura4 his2* [pREP41-GFP-pkl1]	4E	This study
MY990	*h⁺ cut7::bleR pkl1::natR leu1 ura4 his2*	5A	This study
MY1660	*h? cut7::bleR leu1? ura4? his2?*	5B, S7	This study
MY899	*h⁻ cut7::bleR pkl1::natR leu1 ura4*	6A	This study
CH61	*h⁻ wdr8::kanR leu1 ura4*	6A	Our lab stock
MY1616	*h⁻ skf4-1-kanR (nda3-G56D-kanR) cut7-GFP-hphR leu1? ura4? ade6-210?*	6A	This study
MY1618	*h⁻ skf4-2-kanR (nda3-Q334R-kanR) cut7-GFP-hphR leu1? ura4? ade6-210?*	6A	This study
YY173	*h⁻ atb2::ura4⁺ cut7-GFP-kanR leu1 ura4*	6A	This study
YY201	*h⁻ mal3::ura4⁺ cut7-GFP-kanR leu1 ura4*	6A	This study
iHR2239	*h⁺ alp16::kanR leu1 ura4*	6A	Our lab stock
MY986	*h⁻ alp7::ura4+ leu1 ura4*	6A	This study

MY988	*h⁻ alp14::kanR leu1 ura4*	6A	This study
MY1006	*h⁻ dis1::hphR leu1 ura4*	6A	This study
YY68	*h⁻ cut7-22, 68 ade6-210*	S1A	This study
YY70	*h⁻ cut7-22, 70 ade6-210*	S1A	This study
YY71	*h⁻ cut7-22, 71 ade6-210*	S1A	This study
MT31	*h⁻ mal3::kanR leu1 ura4*	S1C	This study
MY1785	*h⁻ skf4-1-kanR (nda3-G56D-kanR) leu1 ade6-210?*	S1C	This study
MY1840	*h⁻ skf5-1 (atb2-G410A) leu1 ade6-210*	S1C	This study
MY1462	*h⁻ klp9-GFP-kanR aur1R-Pnda3-mCherry-atb2 leu1 ura4*	S2A, S2C	This study
MY1464	*h⁻ mal3::ura4⁺ klp9-GFP-kanR aur1R-Pnda3-mCherry-atb2 leu1 ura4*	S2A, S2C	This study
MY1792	*h⁻ alp16::ura4⁺ klp9-GFP-kanR aur1R-Pnda3-mCherry-atb2 leu1 ura4*	S2A, S2C	This study
MY1466	*h⁺ ase1-GFP-kanR aur1R-Pnda3-mCherry-atb2 leu1 ura4 his2*	S2B, S2D	This study
MY1469	*h⁺ mal3::ura4⁺ ase1-GFP-kanR aur1R-Pnda3-mCherry-atb2 leu1 ura4 his2*	S2B, S2D	This study
MY1796	*h⁻ alp16::ura4⁺ ase1-GFP-kanR aur1R-Pnda3-mCherry-atb2 leu1 ura4*	S2B, S2D	This study
MY1470	*h⁻ mal3::ura4⁺ kanR-Palp4-GFP-pkl1 aur1R-Pnda3-mCherry-atb2 leu1 ura4*	S3A-B	This study
MY1508	*h⁻ alp16::ura4⁺ kanR-Palp4-GFP-pkl1 aur1R-Pnda3-mCherry-atb2 leu1 ura4*	S3A-B	This study
MY1485	*h⁻ cut7-22 mal3::ura4⁺ kanR-Palp4-GFP-pkl1 aur1R-Pnda3-mCherry-atb2 leu1 ura4*	S3B	This study
MY1487	*h⁻ cut7-22 alp16::ura4⁺ kanR-Palp4-GFP-pkl1 aur1R-Pnda3-mCherry-atb2 leu1 ura4*	S3B	This study
MY1807	*h⁻ msd1-GFP-kanR aur1R-Pnda3-mCherry-atb2 leu1 ura4*	S3C, S6A	This study
MY1831	*h⁻ alp16::ura4⁺ msd1-GFP-kanR aur1R-Pnda3-mCherry-atb2 leu1 ura4*	S3C	This study
MY1809	*h⁻ cut7-22 msd1-GFP-kanR aur1R-Pnda3-mCherry-atb2 leu1 ura4*	S3C, S6A	This study
MY1834	*h⁻ cut7-22 alp16::ura4⁺ msd1-GFP-kanR aur1R-Pnda3-mCherry-atb2 leu1 ura4*	S3C	This study
MY195	*h⁻ wdr8-GFP-kanR aur1R-Pnda3-mCherry-atb2 leu1 ura4*	S3D, S6B	This study
MY1837	*h⁻ alp16::ura4⁺ wdr8-GFP-kanR aur1::aur1R-Pnda3-mCherry-atb2 leu1 ura4*	S3D	This study
MY1774	*h⁻ cut7-22 wdr8-GFP-kanR aur1::aur1R-Pnda3-mCherry-atb2 leu1 ura4*	S3D, S6B	This study
MY1828	*h⁻ cut7-22 alp16::ura4⁺ wdr8-GFP-kanR aur1::aur1R-Pnda3-mCherry-atb2 leu1 ura4*	S3D	This study
MY1816	*h⁻ kanR-Palp4-GFP-klp2 aur1R-Pnda3-mCherry-atb2 leu1 ura4* [pREP41]	S3D	This study
MY1819	*h⁻ kanR-Palp4-GFP-klp2 aur1R-Pnda3-mCherry-atb2 leu1 ura4* [pREP41-pkl1]	S3D	This study

YY309	*h⁻ klp2::hphR cut12-GFP-ura4⁺ aur1R-Pnda3-mCherry-atb2 leu1 ura4* [pREP41-GFP]	S8	This study
YY311	*h⁻ klp2::hphR cut12-GFP-ura4⁺ aur1R-Pnda3-mCherry-atb2 leu1 ura4* [pREP41-GFP-pkl1]	S8	This study

*Strains were developed for this study unless otherwise specified.

his2=his2-245; *leu1=leu1-32*; *ura4=ura4-D18*.

Figure S1. Yukawa *et al*.

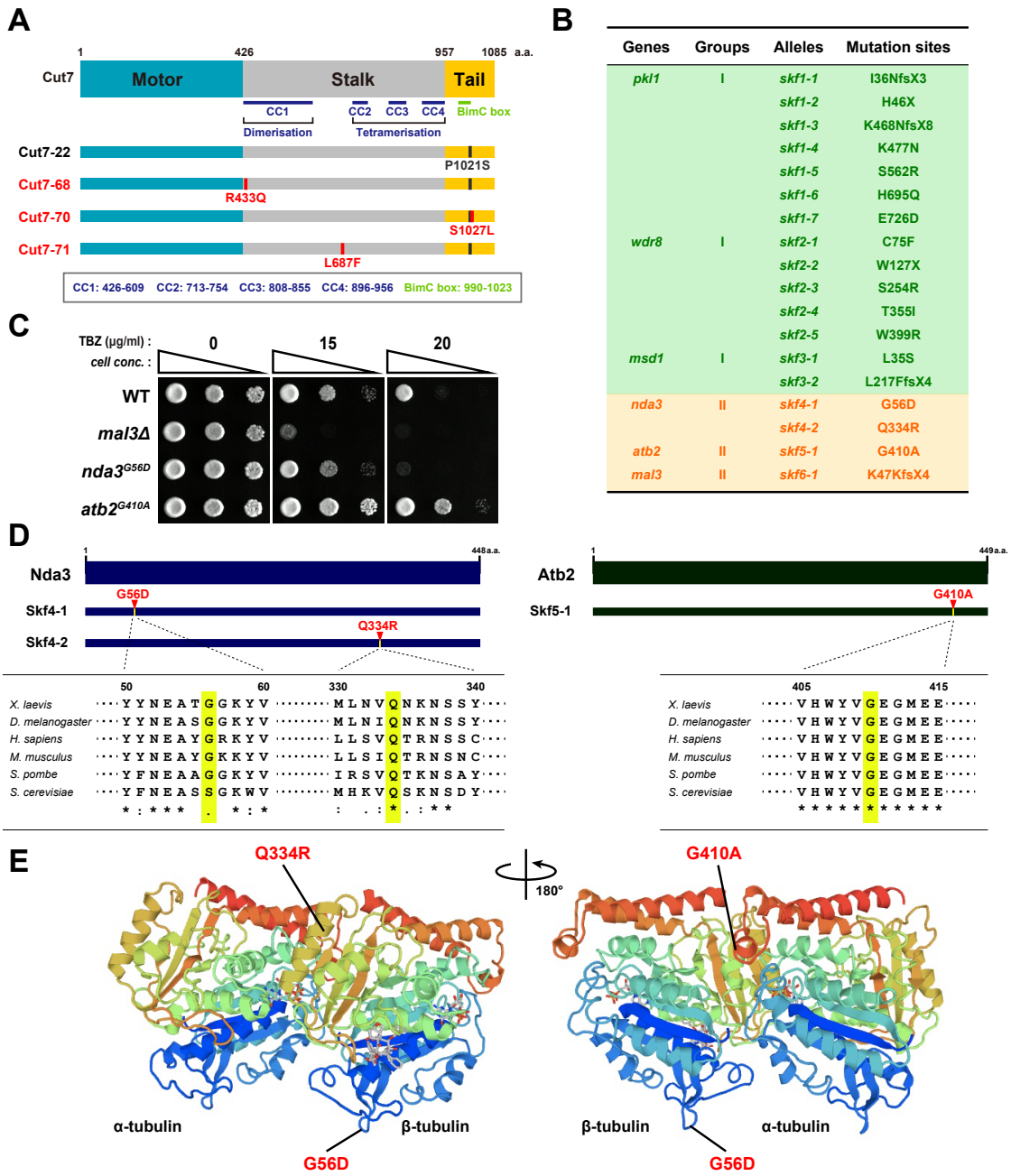

Figure S1. (continued) Yukawa *et al*.

Figure S1. The positions of intragenic mutations and mutated tubulin genes that suppress *cut7-22*
(A) Mutation sites in intragenic suppressors of the *cut7-22* ts mutant. Overall domain structure of Cut7 are shown on the top: the N-terminal motor domain (blue), the medial stalk domain (gray) including multiple coiled-coil regions (CC) and the C-terminal region (yellow) containing the characteristic BimC. The positions of 3 intragenic mutations are also shown. **(B)** A summary table of *skf* mutant alleles and corresponding genes. Group I (*skf1*-*skf3*) shown in green consists of genes encoding the MWP complex, while Group II (*skf4*-*skf6*) shown in orange is composed of those encoding *nda3*, *atb2* and *mal3*. Mutation sites in individual alleles are also provided on the far right corner. X and fs stand for termination codons and frame-shift mutations, respectively. **(C)** Spot test. Indicated strains were spotted onto rich YE5S agar plates in the absence or presence of TBZ (15 μg/ml or 20 μg/ml) and incubated at 30°C for 3 d. 10-fold serial dilutions were performed in each spot. *cell conc.*, cell concentration. **(D)** Mutation sites in *nda3*/*skf4* and *atb2*/*skf5*. Alignments of amino acid sequences corresponding to the regions surrounding mutated amino acid residues (marked with green columns) are also shown on the bottom. **(E)** 3D-simulation of the α-/β-tubulin heterodimer. The positions of the mutated amino acid residues in *nda3*/*skf4* and *atb2*/*skf5* are indicated.

Figure S2. Yukawa *et al*.

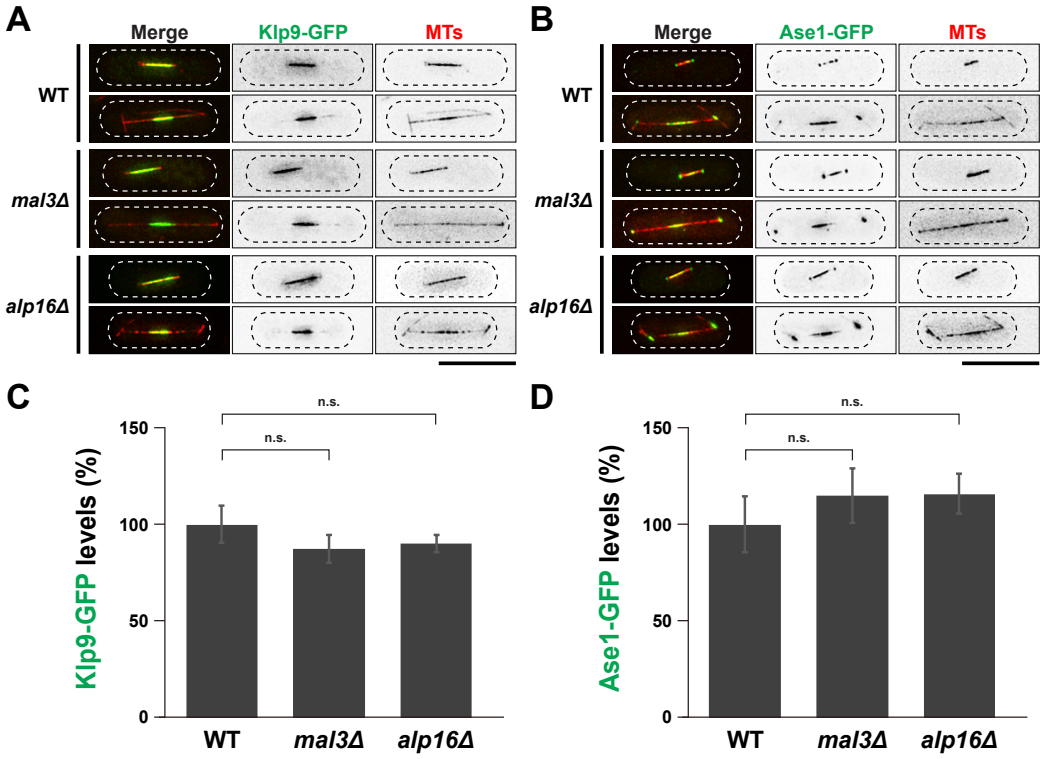

Figure S2. Proper localization of spindle midzone markers in *mal3* or *alp16* deleted cells

(A, B) Representative images of Klp9-GFP (**A**) or Ase1-GFP (**B**). Wild-type, *mal3*Δ or *alp16*Δ cells containing mCherry-Atb2 and Klp9-GFP (**A**) or mCherry-Atb2 and Ase1-GFP (**B**) were grown at 27°C, and images of mitotic cells were taken. **(C, D)** Quantification of Klp9-GFP (**C**) or Ase1-GFP signal intensities (**D**). Fluorescence intensities of Klp9-GFP (**C**) or Ase1-GFP (**D**) on the spindle microtubule were measured. All *p*-values were obtained from the two-tailed unpaired Student's t test. Data are presented as the means ± SE (≥ 21 cells). n.s., not significant.

Figure S3. Yukawa *et al*.

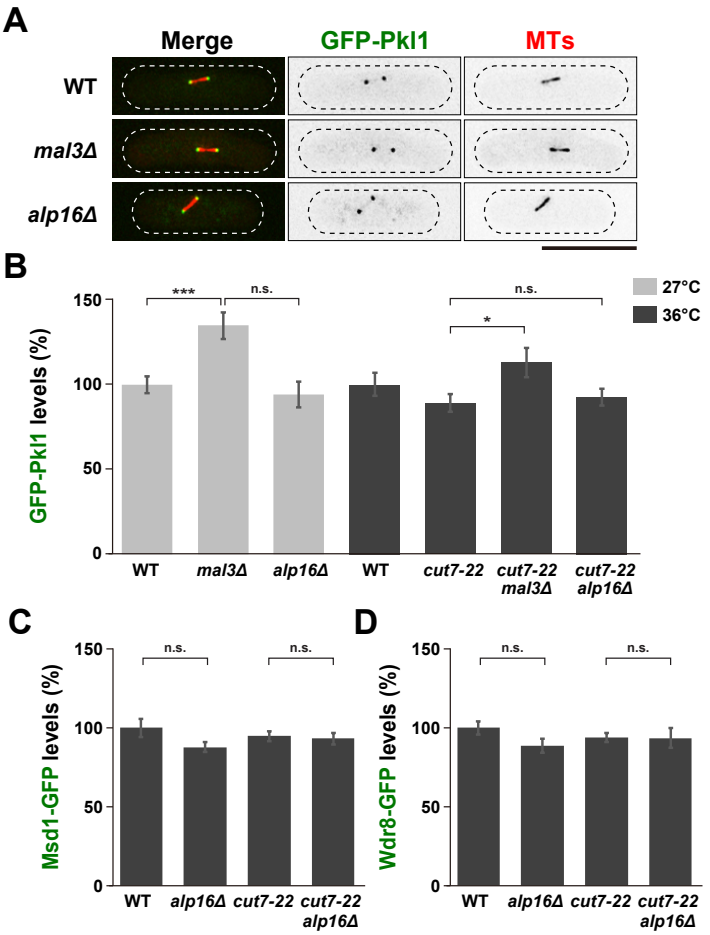

Figure S3. Fluorescence intensities of GFP-Pkl1 in individual strains

(A) Representative images showing mitotic localization of GFP-Pkl1 at the SPB are presented in indicated cells. All strains contain GFP-Pkl1 and mCherry-Atb2. Cells were incubated at 27°C. Scale bar, 10 μm. **(B-D)** Quantification of GFP-Pkl1 (**B**), Msd1-GFP (**C**) or Wdr8-GFP (**D**) intensities at the mitotic SPB. Each cell was incubated at 27°C (**B**) or 36°C for 2 h (**B-D**), and the total values of GFP fluorescence intensities at the SPB were measured. The values of wild-type cells were set as 100% (27°C and 36°C each) and compared to those from other strains under the same condition. All *p*-values were obtained from the two-tailed unpaired Student's t test. Data are presented as the means ± SE (n≥12). *, $P < 0.05$, ***, $P < 0.001$, n.s., not significant.

Figure S4. Yukawa *et al*.

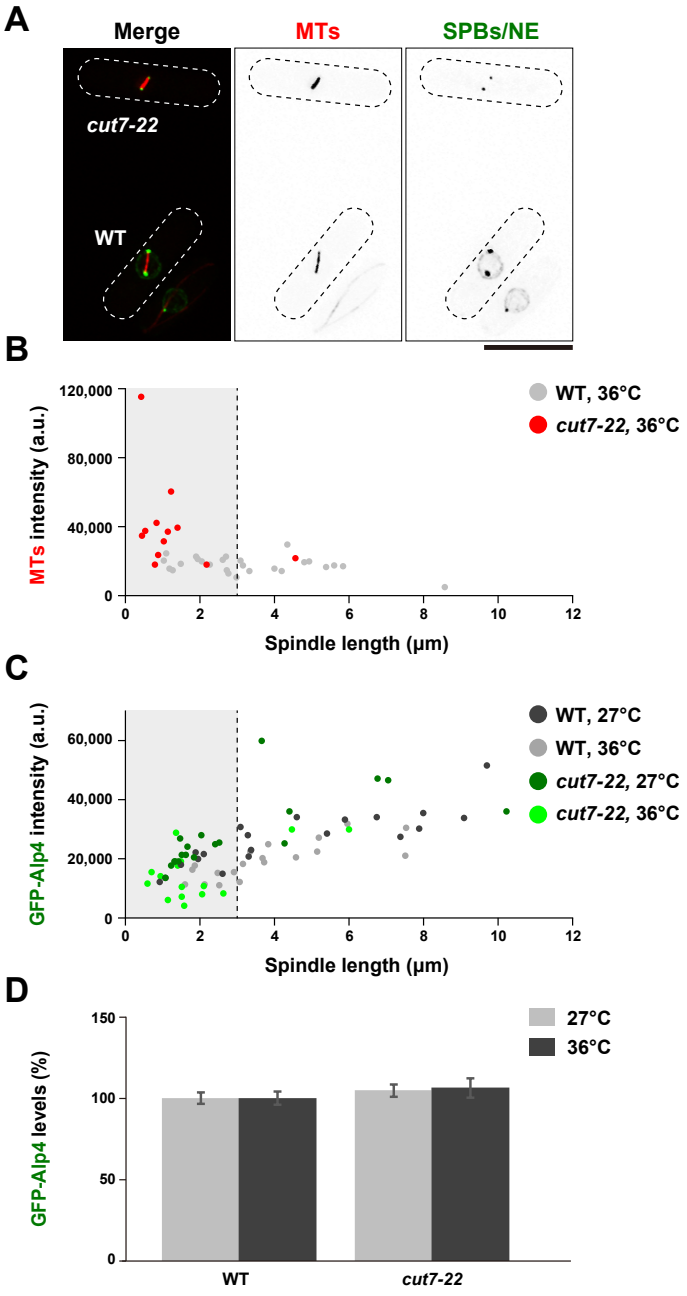

Figure S4. (continued) Yukawa *et al*.

Figure S4. Fluorescence intensities of spindle microtubules and the γ-tubulin complex in *cut7-22* cells
(A) Comparison of intensities of preanaphase spindle microtubules (< 3 μm) between wild-type and *cut7-22* cells in the same field. These two strains were mixed in the same culture, grown at 27°C, shifted to 36°C and further incubated for 2 h. While wild-type cells contain mCherry-Atb2 (MTs), Cut11-GFP (SPB/NE) and GFP-Alp4 (SPB), *cut7-22* cells contain mCherry-Atb2 (MTs) and GFP-Alp4 (SPB). Images of mitotic cells were captured in the same field. Note that SPB signals are brighter in a wild-type cell (lower) than those in a *cut7-22* cell (upper), as the former cell contains Cut11-GFP in addition to GFP-Alp4, thereby wild-type and *cut7-22* cells precisely being assigned. Scale bar, 10 μm. **(B)** Quantification. Fluorescence intensities of spindle microtubules obtained in (**A**) were measured in each strain and plotted in relation to the spindle length. A vertical dotted line represents the spindle length (3 μm) at metaphase. Note that only cells that displayed bipolar (not monopolar) spindles were taken into account. **(C)** Distribution of GFP-Alp4 intensities. Wild-type or *cut7-22* cells containing mCherry-Atb2 and GFP-Alp4 were grown at 27°C. A half of the cultures was shifted to 36°C, while the other half was kept at 27°C. After 2 h incubation, fluorescence intensities of GFP-Alp4 were measured in each strain and plotted in relation to the spindle length (dark- and light-gray circles, wild-type cells at 27°C or 36°C respectively; dark- and light-green circles, *cut7-22* cells at 27°C or 36°C respectively). A vertical dotted line represents the spindle length (3 μm) at metaphase. Note that only cells that displayed bipolar (not monopolar) spindles were taken into account. **(D)** Quantification. Fluorescence intensities of GFP-Alp4 were measured in wild-type or *cut7-22* cells that were incubated at either 27°C or 36°C. The values of wild-type cells incubated at 27°C or 36°C were each set as 100%, and compared to those of *cut7-22* cells under the same condition. Data are presented as the means ± SE (n>30).

Figure S5. Yukawa *et al*.

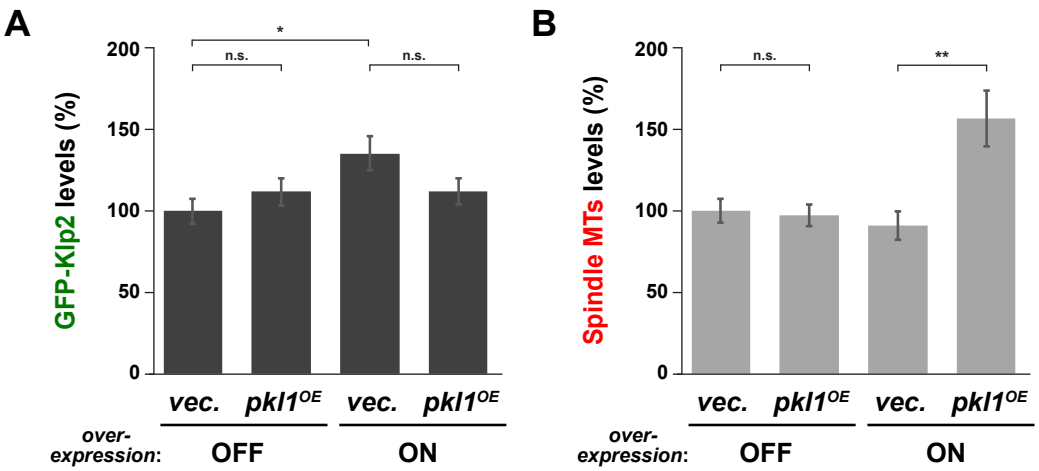

Figure S5. Fluorescence intensities of GFP-Klp2 and spindle microtubules in Pkl1-overproduced cells
(A, B) Wild type cells containing GFP-Klp2 and mCherry-Atb2 were transformed with vector plasmids (*vec.*) or plasmids carrying the thiamine-repressible *nmt41-pkl1*$^{+}$ gene (*pkl1*^{OE}) and grown in the liquid minimal medium in the absence (ON) or presence (OFF) of thiamine for 16 h at 30°C. Under this condition, ~50% of cells contained monopolar spindles. Signal intensities of GFP-Klp2 on the spindles (**A**) and mCherry-Atb2 (spindle microtubules, **B**) were quantified in cells containing bipolar spindles. The levels of spindle microtubule were plotted against the spindle length in individual mitotic cells (**B**). All *p*-values were obtained from the two-tailed unpaired Student's t test. Data are presented as the means ± SD (≥20 cells). **, $P < 0.01$, n.s., not significant.

Figure S6. Yukawa *et al*.

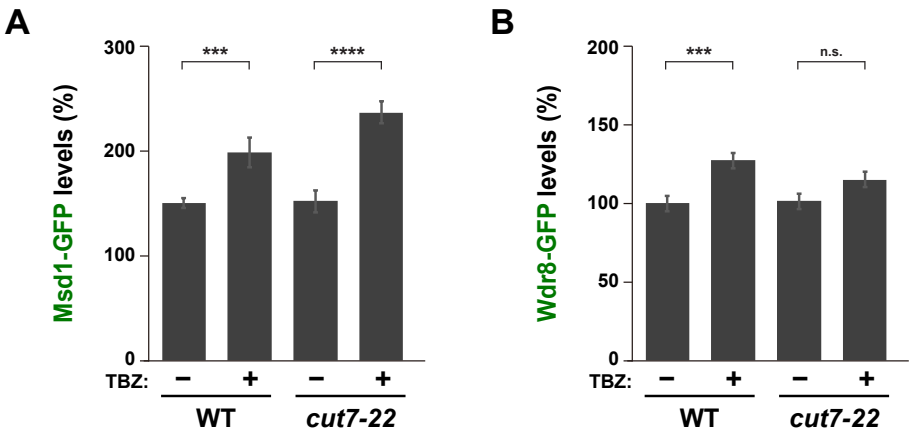

Figure S6. Fluorescence intensities of Msd1-GFP and Wdr8-GFP in *cut7-22* ts cells

(A, B) Fluorescence intensities of Msd1-GFP (**A**) or Wdr8-GFP (**B**) at the mitotic SPB were measured in wild-type and *cut7-22* cells that were incubated at 27°C for 12-16 h in the absence or presence of 20 μg/ml TBZ. All *p*-values were obtained from the two-tailed unpaired Student's t test. Data are presented as the means ± SE (n≥16). ***, P < 0.001, ****, P < 0.0001. n.s., not significant.

Figure S7. Yukawa *et al*.

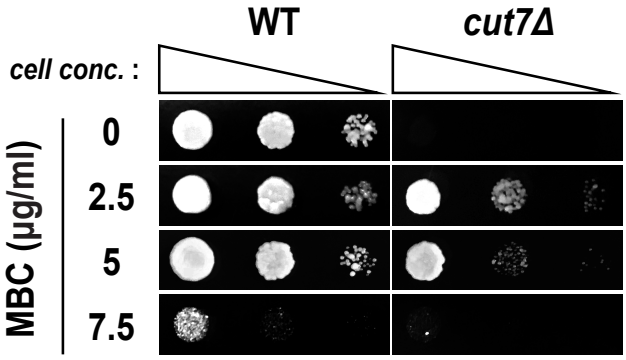

Figure S7. A microtubule-depolymerizing drug, MBC, renders *cut7*Δ cells viable
Spot test. One of wild-type or *cut7*Δ colonies obtained from tetrad dissection shown in Figure 5A were spotted onto YE5S plates in the absence or presence of various concentrations of MBC, and incubated at 27°C for 3 d. *cell conc.*, cell concentration.

Figure S8. Yukawa *et al*.

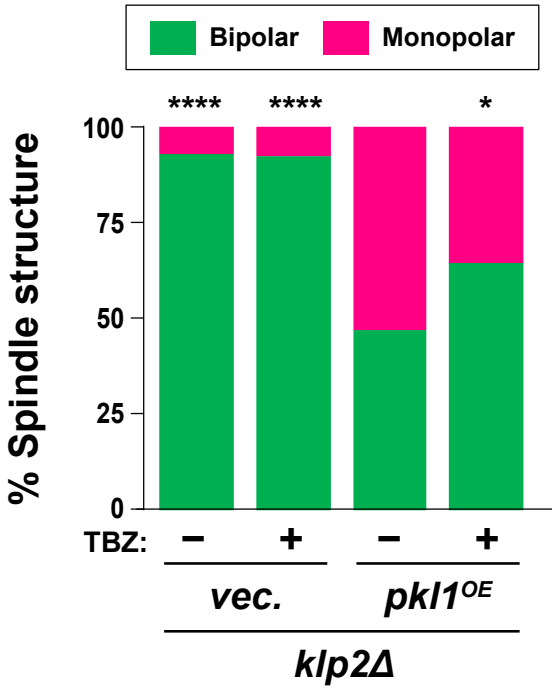

Figure S8. TBZ ameliorates spindle structures in Pkl1-overproduced cells

*klp2*Δ cells containing GFP-Klp2 and mCherry-Atb2 were transformed with vector plasmids (*vec.*) or plasmids carrying the thiamine-repressible *nmt41-GFP-pkl1*$^{+}$ gene (*pkl1*^{OE}) and grown in the liquid minimal medium containing thiamine for 24 h at 30°C in the absence or presence of 20 μg/ml TBZ. The morphology of mitotic spindle microtubules was observed and classified into bipolar (green) or monopolar spindles (magenta). All *p*-values were obtained from the two-tailed χ^2 test. Data are presented as the means ± SE (≥42 cells). *, $P < 0.05$, ****, $P < 0.0001$.